Lattice study of the nucleon excited states with domain wall fermions

Shoichi Sasaki

RIKEN-BNL Research Center, Brookhaven National Laboratory, Upton, New York 11973-5000
and Department of Physics, University of Tokyo, Hongo 7-3-1, Bunkyo-ku, Tokyo 113-0033, Japan

Tom Blum

RIKEN-BNL Research Center, Brookhaven National Laboratory, Upton, New York 11973-5000

Shigemi Ohta

Institute for Particle and Nuclear Studies, KEK, Tsukuba, Ibaraki 305-0801, Japan
and RIKEN-BNL Research Center, Brookhaven National Laboratory, Upton, New York 11973-5000

We present results of our numerical calculation of the mass spectrum for isospin one-half and spin one-half nonstrange baryons, i.e., the ground and excited states of the nucleon, in quenched lattice QCD. We use a new lattice discretization scheme for fermions, domain wall fermions, which possess almost exact chiral symmetry at nonzero lattice spacing. We make a systematic investigation of the negative-parity N^* spectrum by using two distinct interpolating operators at $\beta = 6/g^2 = 6.0$ on a $16^3 \times 32 \times 16$ lattice. The mass estimates extracted from the two operators are consistent with each other. The observed large mass splitting between this state, $N^*(1535)$, and the positive-parity ground state, the nucleon $N(939)$, is well reproduced by our calculations. We have also calculated the mass of the first positive-parity excited state and find that it is heavier than the negative-parity excited state for the quark masses studied.

I. INTRODUCTION

An important challenge in lattice calculations is to reproduce the hadron mass spectrum from first principles in quantum chromodynamics (QCD). The latest lattice QCD calculations of the light-hadron mass spectrum in the quenched approximation agree with experimental values within about 5% [1–3]. However, this success is mainly restricted to ground states. Indeed, results are scarcely available for the excited-state mass spectrum.

Another essential shortcoming of these calculations which use Wilson or Kogut-Susskind fermions is the absence of chiral symmetry at finite lattice spacing, in accord with the Nielsen-Ninomiya no-go theorem [4]. At nonzero lattice spacing Wilson fermions explicitly break the full chiral symmetry of the continuum down to the vector subgroup, so only flavor symmetry is preserved. On the other hand, Kogut-Susskind fermions have only a single exact $U(1)$ axial symmetry, and flavor symmetry is completely broken [5]. Of course, it is expected that in the continuum limit, which is difficult to achieve in practice, both actions recover the full chiral symmetry.

Several years ago Kaplan constructed a new type of lattice fermion [6] known as domain wall fermions, which were further developed by Shamir [7,8] and also by Narayanan and Neuberger [9]. Especially, the former reformulated it for lattice QCD simulations. The key feature of domain wall fermions is that they utilize an extra fifth dimension to circumvent the Nielsen-Ninomiya no-go theorem and maintain chiral symmetry at nonzero lattice spacing. In practical simulations the extra dimension is finite, so the chiral symmetry is not exact. The symmetry breaking is very soft, however, since it is highly suppressed with the number of sites in the

extra dimension, L_s. In other words, L_s gives us a way to control the violation of chiral symmetry. Domain wall fermions also possess exact flavor symmetry for any value of L_s.

Quenched lattice QCD calculations with domain wall fermions have shown that good chiral properties are obtained for moderate sizes of the fifth dimension, $L_s \sim 10 - 16$, if the lattice spacing is small enough ($a \lesssim 0.1$ fm) [10,11]. Recent studies by the RIKEN-BNL–Columbia–KEK Collaboration [12] and the CP-PACS Collaboration [13] have quantified in detail the explicit chiral symmetry breaking effects due to finite L_s. For low energy QCD, the results can be simply summarized: there is a unique additive quark mass, m_{res}, appearing in the low energy QCD Lagrangian which arises from the finite size of the extra dimension [12]. This additive quark mass has been measured quite accurately, and for $L_s = 16$ and quenched $\beta = 6.0$, $m_{res} \approx 3\%$ of the strange quark mass [12,13]. In this paper, we apply domain wall fermions to baryon excited states, especially the spin one-half and isospin one-half negative-parity nucleon, $N^*(1535)$, as a further test of domain wall fermions in the baryon sector. For masses which are $O(1)$ GeV in the chiral limit, we do not expect m_{res} to have a significant effect.

We are interested in a long-standing puzzle in the excited state spectrum of the nucleon. The first question addressed in this paper is whether the mass difference between the nucleon $N(939)$ and the negative-parity nucleon $N^*(1535)$ is well reproduced in lattice QCD. The spin one-half N^* state can be considered the *parity partner* of the nucleon. Of particular interest is the large mass splitting between N and N^*. From the viewpoint of parity partners, these two states would be degenerate if the relevant 2-flavor chiral symmetry were exact and preserved by the vacuum [14]. Of course, there is no proof that this large mass splitting comes directly

from the spontaneous breaking of chiral symmetry. However, at least spontaneous chiral symmetry breaking is responsible for the absence of such parity doubling since the explicit breaking is quite small in the case of two flavors. In this sense, regardless of a model or a theory, *chiral symmetry and its spontaneous breaking* are important for reproducing precisely the mass splitting between parity-partner hadrons. In this paper we show that domain wall fermions accurately reproduce the large observed mass splitting (some of our results have been reported earlier [15,16]).

Conventional lattice fermion schemes have had difficulty in this challenge. An early calculation [17] using Wilson fermions as well as a more recent one [18], both just managed to extract a mass splitting between the parity partners with large uncertainties.[1]

The first sophisticated calculation [19] using an improved Wilson fermion action and relatively heavy quarks resolved a definite mass splitting between the parity partners which, however, was about a factor of two smaller than the observed splitting. Recent results using improved Wilson fermions have confirmed the large mass splitting over a wide range of quark masses that we have found with domain wall fermions [20,21]. We note that the leading lattice spacing errors that are removed from these improved calculations break chiral symmetry. Although Kogut-Susskind fermions have a remnant $U(1)$ axial symmetry, they cannot be used practically for the spin one-half N^* mass calculation due to flavor mixing. The reason is that Kogut-Susskind fermions have only discrete flavor symmetries belonging to a subgroup of $SU(4)$ [5] which contains three irreducible representations, **8**, **8**′ and **16** for baryon operators. Two appropriate representations **8** and **16**, to which $N^*(1535)$ belongs, also contain the negative-parity Λ states $\Lambda(1405)$ and $\Lambda(1520)$ and the spin three-half negative-parity nucleon state $N^*(1520)$ [5]. Thus, the study of the spin one-half N^* spectrum with Kogut-Susskind fermions always faces inevitable contamination from lower mass states.

It is also interesting to note that a non-relativistic quark model with the so-called color magnetic interaction [22] and the MIT bag model [23], both of which explicitly break chiral symmetry, have some difficulty reproducing the large mass splitting between $N(939)$ and $N^*(1535)$ without adoption of less realistic model parameters. The non-relativistic quark model is based on a harmonic oscillator description of the orbital motion of constituent quarks. As remarked in the appendix of the original paper by Isgur and Karl [22], the plausible value of its oscillator quantum should be roughly 250 MeV to reproduce the observed charge radius and magnetic moment of the nucleon. Since this model regards $N^*(1535)$ as a state with one quantum excitation in orbital motion, it indicates that the corresponding N^* state lies at most a few hundred MeV above the ground state. Even

worse, there is the serious problem of the wrong ordering between $N^*(1535)$ and the positive-parity excited nucleon $N'(1440)$ because the corresponding N' state should be assigned two oscillator quanta in this model [22]. This wrong ordering problem does not seem to be easily alleviated [24]. It is easy to see that the MIT bag model faces essentially the same problem, as the single quark states in the model alternate in parity with roughly even spacings [23].

The question arises how does this ordering of N^* and N' appear in lattice QCD calculations? Until [15] this question could not be answered for lack of systematic results and investigations. A calculation of the mass of the positive-parity excited nucleon is, of course, much more difficult than the nucleon ground state. Attempts have been made to evaluate the N' mass from a two state fit to the nucleon correlation function [25]. However, large statistics are required compared to a single exponential fit. Also it is difficult to control the systematic errors. Leinweber used the QCD sum rule (QCDSR) continuum model and quenched lattice data to estimate the threshold of contributions from excited states [26]. However, the scaling of his result has been questioned by Allton and Capitani [27]. In this paper we take an alternative approach, using the continuum-like behavior of the domain wall fermion operator [15] to obtain the mass of the positive-parity excited nucleon. Our results have been confirmed in [20] where a similar approach is employed in the context of improved Wilson fermions.

In conventional lattice QCD calculations an interpolating operator which is strongly associated with the non-relativistic limit is used to extract the mass of the nucleon ground state. A second unconventional operator, which does not have a non-relativistic limit, is discarded since it is expected to couple weakly to the ground state. Indeed, using this operator, no one has succeeded in evaluating the mass of the nucleon ground state in lattice QCD calculations with Wilson fermions [28] because of its small coupling to the ground state [26]. The expectation of an approximately zero overlap on the ground state provides the possibility that the use of the second operator in lattice calculations directly yields the mass of the N' state, at least in the relatively heavy (valence) quark mass region. This prospect, however, is built on the assumption that the lattice defined operators inherit the features of the continuum ones. In the case of the Wilson fermions, the Wilson term, which explicitly breaks chiral symmetry, induces mixing between the conventional and unconventional operators [29,26]. Thus, the desired feature of the unconventional operator in the continuum is diminished in lattice calculations with Wilson fermions. On the other hand, this type of mixing between three quark operators is absent at one loop in perturbation theory using domain wall fermions with large L_s [30]; thus we expect this mixing to be suppressed in domain wall fermion lattice calculations. Indeed, we find that the second operator has negligible overlap with the ground state and furthermore provides a reliable signal of the excited state as the asymptotic state in the heavy quark mass region.

The organization of our paper is as follows. In Sec. II, we briefly review the basic formulas and notation regarding domain wall fermions. In Sec. III we investigate the properties

---

[1]In a recent report [40] which appeared after this work was complete it is clear that the chiral symmetry of their fermions was significantly improved by simulating closer to the continuum limit than previous studies which used Wilson fermions and by adding the clover term.

of the two-point correlation function for the nucleon and its parity partner. Section IV gives the details of our Monte Carlo simulations and the results for the parity partner of the nucleon (N^*) and the first positive-parity excited nucleon (N'). Then, we compare our results to the experimental values. Finally, we present our conclusions in Sec. V.

II. DOMAIN WALL FERMIONS

In this section we closely follow the development of domain wall fermions by Shamir [7,8]. The domain wall fermion action is essentially regarded as a five-dimensional extension of the Wilson fermion action:

$$S_{\text{DWF}} = -\sum_{x,x'} \sum_{s,s'} \bar{\Psi}(x,s)[\delta_{s,s'}D^{\parallel}_{x,x'} + \delta_{x,x'}D^{\perp}_{s,s'}]\Psi(x',s'),$$

$$(1)$$

where x,x' are four-dimensional Euclidean space-time coordinates and s,s' denote coordinates in the extra dimension labeled from 0 to L_s-1 (to take advantage of existing high-speed computer code, our domain wall fermion Dirac operator is the Hermitian conjugate of the one in [8], hence our notation is the same as in [12]). Here, $D^{\parallel}_{x,x'}$ corresponds to the four-dimensional Wilson-Dirac operator with a mass term (domain wall height) M_5:

$$D^{\parallel}_{x,x'} = \frac{1}{2} \sum_{\mu} \{(1-\gamma_{\mu})U_{\mu}(x)\delta_{x+\hat{\mu},x'} + (1+\gamma_{\mu})$$

$$\times U^{\dagger}_{\mu}(x')\delta_{x-\hat{\mu},x'}\} + (M_5-4)\delta_{x,x'},$$

$$(2)$$

where the Wilson term and mass term have opposite relative sign compared to the conventional one. $D^{\perp}_{s,s'}$ is the five-dimensional analogue of the four dimensional Wilson hopping term with γ_{μ} replaced by γ_5 and $U_5(x,s)=1$:

$$D^{\perp}_{s,s'} = \frac{1}{2}\{(1-\gamma_5)\delta_{s+1,s'} + (1+\gamma_5)\delta_{s-1,s'} - 2\delta_{s,s'}\}$$

$$-\frac{m_f}{2}\{(1-\gamma_5)\delta_{s,L_s-1}\delta_{0,s'} + (1+\gamma_5)\delta_{s,0}\delta_{L_s-1,s'}\}.$$

$$(3)$$

Note that the five dimensional fermions $\Psi(x,s)$ are coupled only to four-dimensional gauge fields. The boundaries $s=0$ and $s=L_s-1$ are anti-periodic and coupled with a weight m_f.

For an appropriate choice of M_5, this action has two chiral zero modes of opposite handedness, one localized on each boundary of the fifth dimension. To simulate low energy QCD, four dimensional quarks are interpolated from the chiral modes:

$$q(x) = P_L\Psi(x,0) + P_R\Psi(x,L_s-1),$$

$$(4)$$

$$\bar{q}(x) = \bar{\Psi}(x,L_s-1)P_L + \bar{\Psi}(x,0)P_R,$$

$$(5)$$

where $P_{R,L} = (1\pm\gamma_5)/2$. With this definition, one can see that the m_f terms in $D^{\perp}_{s,s'}$ directly yield the usual four dimensional explicit chiral symmetry breaking term, $m_f\bar{q}(x)q(x)$, on the four dimensional layers $s=0$ and $s=L_s-1$. The above definition of the quark fields is the simplest one but is not unique.

In the free theory, for the choice $0<M_5<2$, the domain wall fermion action corresponds to one flavor, and the four-dimensional light quark mass is given as $m_q = m_f M_5(2-M_5)$ in the limit $L_s\to\infty$ and $m_f\to0$. This situation is approximately unchanged in lattice QCD simulations if M_5 is simply shifted, $M_5\to M_5-M_c$ [10], where a simple estimate of M_c is given in terms of the critical hopping parameter for four-dimensional Wilson fermions [31].

In the case of domain wall fermions, the $SU(N_f)$ axial transformation can be defined vectorially [8] as

$$[\mathcal{Q}^a_A,\Psi(x,s)] = +i\epsilon(s)\lambda^a\Psi(x,s),$$

$$(6)$$

$$[\mathcal{Q}^a_A,\bar{\Psi}(x,s)] = -i\epsilon(s)\bar{\Psi}(x,s)\lambda^a,$$

$$(7)$$

where $\Psi(x,s)$ is a five-dimensional zero mode. Opposite axial charges are assigned to fermions in the two half-spaces, so $\epsilon(s)=1$ for $0\leq s<L_s/2$ and $\epsilon(s)=-1$ for $L_s/2\leq s\leq L_s-1$. The reason for this is clear: left and right handed modes are globally separated in the extra dimension.

With this axial transformation on the five dimensional fields, the four dimensional quark fields obey the familiar axial transformation:

$$[\mathcal{Q}^a_A,q(x)] = +i\gamma_5\lambda^a q(x),$$

$$(8)$$

$$[\mathcal{Q}^a_A,\bar{q}(x)] = -i\bar{q}(x)\gamma_5\lambda^a.$$

$$(9)$$

In general the domain wall fermion action is not invariant under the transformations (6) and (7) in the limit $m_f=0$ because of a non-vanishing divergence of the axial current on the intermediate layers $s=L_s/2-1$ and $s=L_s/2$ which gives rise to an extra pseudoscalar density in the axial Ward-Takahashi identity [8]. However, such an anomalous term, which provides a chiral symmetry breaking effect due to mixing of the left- and right-handed modes, vanishes as $L_s\to\infty$ [8].

Theoretically, this residual breaking effect can be described by an additive quark mass m_{res} in the four-dimensional low energy effective Lagrangian for QCD [12], and recent simulations, in which m_{res} was determined in several ways, appear to confirm this [12]. Simulations also show that for sufficiently small lattice spacing, $m_{\text{res}}\to0$ as $L_s\to\infty$, and at the very least, m_{res} is small and accurately known for a wide range of L_s [12,13]. Thus, in this study we will henceforth ignore these small effects and assume the chiral limit is $m_f=0$ instead of $m_f=-m_{\text{res}}$. Finally, we note that the non-perturbative origin of these effects and their relation to certain non-perturbative gauge field configurations is a very interesting and active area of research [32].

III. BARYON SPECTRUM

A. Baryon two-point correlator

The mass m_B of the low-lying baryon B can be extracted from the two-point correlation function composed of the baryon interpolating operator $\mathcal{O}_B$, which has the appropriate quantum numbers specified by the desired state. Let us consider the vacuum expectation value of the time-ordered product of interpolating operators. The Euclidean time correlation function is projected out at zero spatial momentum through the sum over $\vec{x}$:

$$G_{\mathcal{O}_B}(t) = \sum_{\vec{x}} \langle 0|T\{\mathcal{O}_B(\vec{x},t)\bar{\mathcal{O}}_B(0,0)\}|0\rangle, \qquad (10)$$

which is dominated by the contribution of the lowest mass state for large Euclidean time, $G_{\mathcal{O}_B}(t) \sim \exp(-M_B|t|)$. For a spin one-half baryon, of course, the correlation function has non-trivial Dirac structure which may be expressed in the form

$$G_{\mathcal{O}_B}(t) \xrightarrow{\text{large } t} (1+\gamma_4)\theta(t)A_B e^{-M_B t}$$
$$+ (1-\gamma_4)\theta(-t)A_B e^{+M_B t}, \qquad (11)$$

where the positive definite A_B is proportional to the square of the coupling strength between the interpolating operator $\mathcal{O}_B$ and the lowest mass state. The first and second terms are *particle* and *anti-particle* contributions, respectively. It is easy to get only the particle contribution by taking the trace with the projection operator $P_+ = (1+\gamma_4)/2$, which we abbreviate as $\langle\langle \mathcal{O}_B(t)\bar{\mathcal{O}}_B(0)\rangle\rangle = \mathrm{Tr}\{P_+ G_{\mathcal{O}_B}(t)\}$ hereafter.

B. Interpolating operators

Let us focus on the nucleon channel specified by the spin one-half iso-doublet nonstrange baryons. In order to project out the desired channels, we have to construct interpolating operators from the quark fields with the appropriate quantum numbers ($J=1/2$ and $I=1/2$). However, there is considerable freedom in choosing the specific form of the composite operators. Indeed, there are two possible interpolating operators for the $J^P = 1/2^+$ state, even if we restrict them to contain no derivatives and to belong to the $(\frac{1}{2},0)\oplus(0,\frac{1}{2})$ chiral multiplet under $SU(2)_L \otimes SU(2)_R$ [33,34]:

$$B_1^+(x) = \varepsilon_{abc}[u_a^T(x)C\gamma_5 d_b(x)]u_c(x), \qquad (12)$$

$$B_2^+(x) = \varepsilon_{abc}[u_a^T(x)C d_b(x)]\gamma_5 u_c(x), \qquad (13)$$

where abc and ud have usual meanings as color and flavor indices. C is the charge conjugation matrix and the superscript T denotes transpose. Here, Dirac indices have been suppressed. In Eqs. (12) and (13), the superscript "$+$" refers to positive parity since these operators transform as $\mathcal{P}B_{1,2}^+(\vec{x},t)\mathcal{P}^\dagger = +\gamma_4 B_{1,2}^+(-\vec{x},t)$ under parity. To be precise,

the linear combinations $B_1^+ \pm B_2^+$ belong to distinct $(\frac{1}{2},0) \oplus (0,\frac{1}{2})$ chiral multiplets under $SU(2)_L \otimes SU(2)_R$ [33,34].

The operator B_1^+ alone is usually used in lattice QCD calculations to extract the nucleon ground state since B_2^+ couples only weakly to the ground state due to its vanishing in the non-relativistic limit [26]. In fact, nobody has succeeded in extracting the nucleon mass spectrum from the B_2^+ operator. In our calculation, we also confirm that the ground state cannot be extracted from $\langle\langle B_2^+(t)\bar{B}_2^+(0)\rangle\rangle$; however, we have had some success with respect to the excited-state mass spectrum which we discuss in Sec. IV C.

Multiplying the left hand side of the previous positive-parity operators by γ_5, we obtain the interpolating operators with negative parity, $J^P = 1/2^-$ [19]:

$$B_1^-(x) = \gamma_5 B_1^+(x) = \varepsilon_{abc}[u_a^T(x)C\gamma_5 d_b(x)]\gamma_5 u_c(x), \qquad (14)$$

$$B_2^-(x) = \gamma_5 B_2^+(x) = \varepsilon_{abc}[u_a^T(x)C d_b(x)]u_c(x), \qquad (15)$$

since $\mathcal{P}B_{1,2}^-(\vec{x},t)\mathcal{P}^\dagger = -\gamma_4 B_{1,2}^-(-\vec{x},t)$. The important point to notice is the relation between the correlation functions of opposite parities,

$$G_{B^+}(t) = -\gamma_5 G_{B^-}(t)\gamma_5, \qquad (16)$$

since $B_{1,2}^- = \gamma_5 B_{1,2}^+$. Equation (16) means that the two-point correlation function of the spin one-half baryon can couple to both positive- and negative-parity states. Thus, the general form of the two point function is [35]

$$G_{B^+}(t) = (1+\gamma_4)\theta(t)A_{B^+}e^{-M_{B^+}t}$$
$$+ (1-\gamma_4)\theta(-t)A_{B^+}e^{+M_{B^+}t}$$
$$- (1+\gamma_4)\theta(-t)A_{B^-}e^{+M_{B^-}t}$$
$$- (1-\gamma_4)\theta(t)A_{B^-}e^{-M_{B^-}t}. \qquad (17)$$

Note that the backward propagating contributions correspond to the anti-particles of the forward propagating states with opposite parity. The desired state is obtained by choosing the appropriate projection operator, $1 \pm \gamma_4$, and direction of propagation.

Next, consider a lattice with finite extent T in the time direction and (anti-)periodic boundary conditions. Equation (17) is replaced by

$$G_{B^+}(t) = (1+\gamma_4)A_{B^+}e^{-M_{B^+}t} \pm (1-\gamma_4)A_{B^+}e^{-M_{B^+}(T-t)}$$
$$\mp (1+\gamma_4)A_{B^-}e^{-M_{B^-}(T-t)}$$
$$- (1-\gamma_4)A_{B^-}e^{-M_{B^-}t}, \qquad (18)$$

where the (lower) upper sign stands for (anti-)periodic boundary condition on $0 < t < T$. The anti-particle of the opposite-parity state can propagate through the time direction boundaries, so one faces unwanted contamination from the opposite-parity state in extracting the mass of the desired state. This contamination is not unavoidable if a double ex-

ponential fit is used. However, such fits require very high statistics. This is not a serious issue in the measurement of the nucleon ground state since the contamination from the negative-parity nucleon is expected to be negligible due to the large mass splitting $M_{B^-} - M_{B^+}$. Of course, this same splitting does affect the extraction of M_{B^-}. The problem is resolved by choosing appropriate boundary conditions in the time direction to prevent the wrap-around effect, or by increasing the time extent T sufficiently and placing the interpolating operators far from the boundary. In this study we take the former approach. It is common to employ Dirichlet boundary conditions where link valuables in the time direction at $t=0$ and $t=T-1$ are set to zero when calculating quark propagators (for example, see [19]). However, we use a linear combination of two quark propagators with periodic and anti-periodic boundary conditions in the time direction to produce forward propagating states. Although our approach requires two times as many fermion matrix inversions to calculate one quark propagator, it does not suffer from (unknown) reflection effects at the time boundaries induced by Dirichlet boundary conditions.

C. Chiral symmetry and parity doubling

At the end of this section, let us briefly review how unbroken chiral symmetry imposes parity doubling in the hadron spectrum [14,34]. We will generalize the following argument in the Appendix. For the sake of simplicity, we consider a particular transformation of the $SU(2)$ chiral symmetry, $[\mathcal{Q}_A, u] = +i\gamma_5 u$ and $[\mathcal{Q}_A, d] = -i\gamma_5 d$. Then, one can easily find that the two-point correlators $B_1^{\pm}$ and $B_2^{\pm}$ transform as

$$[\mathcal{Q}_A, B_{1,2}^{\pm}(x)\bar{B}_{1,2}^{\pm}(0)] = i\{\gamma_5, B_{1,2}^{\pm}(x)\bar{B}_{1,2}^{\pm}(0)\} \quad (19)$$

in the chiral limit. Now suppose that the vacuum possesses chiral symmetry: $\mathcal{Q}_A|0\rangle = 0$. According to Eq. (19), the two-point correlation functions anti-commute with γ_5,

$$\{\gamma_5, G_{B^{\pm}}(t)\} = 0. \quad (20)$$

Immediately, with the help of Eq. (16), one finds

$$G_{B^+}(t) = G_{B^-}(t), \quad (21)$$

which means that parity doubling arises in the nucleon channel due to chiral symmetry [34]. Of course, in the real world chiral symmetry is spontaneously broken, $\mathcal{Q}_A|0\rangle \neq 0$, so that such parity doubling does not occur in the actual spectrum [14]. In this sense, the spontaneous breaking of chiral symmetry is responsible for the absence of parity doubling. Thus, it seems important to properly handle chiral symmetry and its spontaneous breaking in order to calculate precisely the mass splitting between the nucleon and its parity partner. Finally, it is important to note that above argument ignores possible consequences to the 't Hooft anomaly condition [36,37].

IV. NUMERICAL RESULTS

A. Computational details

We generate quenched QCD configurations on a $16^3 \times 32$ lattice with the standard single-plaquette Wilson action at $\beta = 6/g^2 = 6.0$. The quark propagator is calculated using domain wall fermions with a fifth dimension of $L_s = 16$ sites and a domain wall height $M_5 = 1.8$. Additional details of the simulation can be found in [12,38]. Quenched $\beta = 6.0$ corresponds to a lattice cutoff of $a^{-1} \approx 1.9$ GeV from $aM_\rho = 0.400(8)$ in the chiral limit and spatial size $La \approx 1.7$ fm [12,38].

We work in Coulomb gauge and calculate quark propagators using wall sources and local sinks. We expect that the use of wall sources provides better overlap with the desired states. To extract the state with desired parity in the spin one-half baryon spectrum, we construct forward (backward) propagating quarks by taking the appropriate linear combination of propagators with periodic and anti-periodic boundary conditions in the time direction, as mentioned before. This procedure eliminates the backward (forward) propagating opposite parity state which wraps around the time boundary.

In addition, we use two sources for quark propagators on each configuration ($t_{\text{src}} = 5$ and $t'_{\text{src}} = 27$) to increase statistics. After the appropriate parity projections, the correlation functions of the corresponding nucleon state can be folded together (averaged as a function of distance from the respective source). Here, time-slices are labeled from 0 to 31. To be clear, we give the form of the nucleon two-point function with arbitrary source location t_{src} after eliminating the unwanted contributions across time boundaries:

$$G_{B^+}(t - t_{\text{src}}) = \begin{cases} (1+\gamma_4)A_{B^+}e^{-M_{B^+}(t-t_{\text{src}})} - (1-\gamma_4)A_{B^-}e^{-M_{B^-}(t-t_{\text{src}})} & (T>t>t_{\text{src}}), \\ (1-\gamma_4)A_{B^+}e^{-M_{B^+}(t_{\text{src}}-t)} - (1+\gamma_4)A_{B^-}e^{-M_{B^-}(t_{\text{src}}-t)} & (t_{\text{src}}>t>0), \end{cases} \quad (22)$$

which is constructed with the positive-parity interpolating operator (either B_1^+ or B_2^+). In the time range $T>t>t_{\text{src}}$, positive- and negative-parity nucleon states are propagating only forward in time. This means that there are only particle contributions in this region. Thus, $P_{\pm} = (1 \pm \gamma_4)/2$ project out positive- and negative-parity states, respectively. Alternatively, for $t_{\text{src}}>t>0$ only the anti-particles contribute to the correlation function. In this case, $P_{\pm}$ act in the opposite way to the former case. In either case, all we have to do is calculate either G_{B^+} or G_{B^-} to extract the masses for both

TABLE I. Single exponential fit of π and ρ two-point correlators at $\beta = 6.0$ on a $16^3 \times 32 \times 16$ lattice with $M_5 = 1.8$. The masses for $am_f < 0.05$ agree within errors with those given in Ref. [12] which were calculated from different correlation functions on a slightly different set of configurations.

am_f	aM_π	aM_ρ	M_π/M_ρ	No. of configs.
0.020	0.2687(24)	0.4530(62)	0.593(14)	98
0.030	0.3224(21)	0.4814(45)	0.670(11)	98
0.040	0.3691(19)	0.5126(42)	0.720(10)	98
0.050	0.4116(18)	0.5395(36)	0.763(8)	98
0.075	0.5080(17)	0.6088(38)	0.834(8)	98
0.100	0.5962(18)	0.6797(36)	0.877(7)	98
0.125	0.6774(17)	0.7483(33)	0.905(6)	98

positive- and negative-parity states since we already know $\mathrm{Tr}\{P_\pm G_{B^+}(t)\} = -\mathrm{Tr}\{P_\mp G_{B^-}(t)\}$ with the help of Eq. (16). In fact, we verified this relation on each configuration and then used $G_{B_1^+}$ and $G_{B_2^-}$ to extract masses.

In our analysis, we use correlation functions in the ranges $t > 5$ and $t < 27$, for the sources $t_{\mathrm{src}} = 5$ and $t'_{\mathrm{src}} = 27$, respectively. After folding the propagators together as described above, we use a single offset from the source, t, defined in the range $0 < t < 27$.

We use 405 independent gauge configurations for the lightest two quark masses, $m_f = 0.02$ and 0.03, 305 configurations for the intermediate ones, $m_f = 0.04$ and 0.05, and 105 configurations for the heavier ones, $m_f = 0.075 - 0.125$. These bare quark masses correspond to mass ratios $M_\pi/M_\rho \approx 0.59 - 0.90$ as shown in Table I. In this calculation, $SU(2)$-isospin symmetry is enforced by equating $m_f = m_f^{(u)} = m_f^{(d)}$, so that the flavor index will not be explicitly displayed hereafter. All calculations were done on the 600 Gflops QCDSP machine at the RIKEN-BNL Research Center.

B. Parity partner of nucleon: N*

We first calculate the effective masses M_{eff} to find appropriate time ranges for fitting. The effective mass is defined by

$$M_{\mathrm{eff}}(t) = \ln\{C(t)/C(t+1)\}, \qquad (23)$$

where $C(t)$ stands for $\langle\langle B_{1,2}^\pm(t) \bar{B}_{1,2}^\pm(0)\rangle\rangle$. We look for a plateau, or time independent region, in this quantity to extract the ground state mass. For example, Figs. 1(a)–1(c) show effective masses for the nucleon (B_1^+) and its parity partner ($B_{1,2}^-$) at $m_f = 0.03$, 0.05, and 0.10. In Fig. 1, the effective mass plot shows a clear plateau for the N, and one that is not as good for the heavier N^*. Statistical uncertainties in Fig. 1 are estimated by a single elimination jack-knife method. The effective masses for the N^* from both $\langle\langle B_1^-(t) \bar{B}_1^-(0)\rangle\rangle$ and $\langle\langle B_2^-(t) \bar{B}_2^-(0)\rangle\rangle$ agree well with each other for all three quark masses, except for $m_f = 0.03$ and $t \lesssim 6$ where there is a small difference outside of statistical errors.

In Fig. 1(a), the effective mass for the N^* becomes so noisy after $t = 9$ that the value of the two-point correlator is

consistent with zero within large errors, so we have left these points off of the plot. In addition, the effective mass shows a steep rise with increasing uncertainty as t increases. This rise in the N^* effective mass weakens at relatively heavy quark masses where the signal becomes stable over 12 time slices.

Next we present mass estimates of the N and N^* obtained from covariant single exponential fits to the corresponding correlators. We fit each correlator from some minimum time slice, t_{min}, to an appropriate maximum time slice ($t_{\mathrm{max}} = 20$ for the N and $t_{\mathrm{max}} = 10 - 15$ for the N^*). t_{max} is roughly fixed with reference to the effective mass calculation. To keep fitting ranges as wide as possible, t_{min} is reduced from $t_{\mathrm{max}} - 2$ until $\chi^2/N_{\mathrm{DF}} > 1.5$ where N_{DF} denotes the degrees of freedom in the fit. Fitting details are given in Tables II–IV. All of our fits have a confidence level larger than 0.2 and estimates from the weighted average of the effective mass agree with the fitted masses within errors. A summary of our N and N^* masses is given in Tables II–IV.

We can roughly estimate the systematic error coming from the choice of fitting range by varying t_{min}. Let us determine the difference between our final fits and fits where the smallest time slice is not included. In the case of B_1^+ (the nucleon), resulting errors are much smaller than the statistical errors of the final fits. On the other hand, for both B_1^- and B_2^-, the estimated systematic errors are comparable to the statistical errors, while for B_1^- at $m_f = 0.04$ and 0.05 the systematic error is a factor of two larger than the statistical one. This uncertainty is directly related to the rise of the N^* effective mass, or poor plateau, in those cases where the correlation function was not statistically well resolved at larger times. This, in turn, has forced us to extract masses from the smaller t region which may be contaminated by excited states.

In Fig. 2 we show the low-lying nucleon spectrum as a function of the quark mass, m_f. The nucleon mass is extracted from B_1^+. We omit the point at $m_f = 0.02$ for the operator B_2^- since a good plateau in the effective mass plot is absent. The N^* mass estimates from $\langle\langle B_1^-(t) \bar{B}_1^-(0)\rangle\rangle$ and $\langle\langle B_2^-(t) \bar{B}_2^-(0)\rangle\rangle$ agree with each other within errors in the whole quark mass range, as expected from their common quantum numbers [15]. Note that this result disagrees with that obtained in [19]: we find no discrepancy between masses extracted from $\langle\langle B_1^-(t) \bar{B}_1^-(0)\rangle\rangle$ and $\langle\langle B_2^-(t) \bar{B}_2^-(0)\rangle\rangle$. However, recent results in [20] and [21] are in good agreement with ours. We also obtain the same mass for the N^* from a mixed correlator $\langle\langle B_1^-(t) \bar{B}_2^-(0) + B_2^-(t) \bar{B}_1^-(0)\rangle\rangle$.

The most remarkable feature in Fig. 2, which was first reported in [15], is that the N-N^* mass splitting is observed over the whole range of quark mass values and grows as the quark mass is decreased. To illustrate this point clearly, we compare two mass ratios in Fig. 3, one from the baryon parity partners M_{N*}/M_N and the other from pseudo-scalar and vector mesons M_π/M_ρ. Experimental points [39] are marked with stars, corresponding to nonstrange (left) and strange (right) sectors. In the strange sector we use Σ^+ and $\Sigma(1750)$ as baryon parity partners and K and K^* for the mesons. The baryon mass ratio clearly grows with decreas-
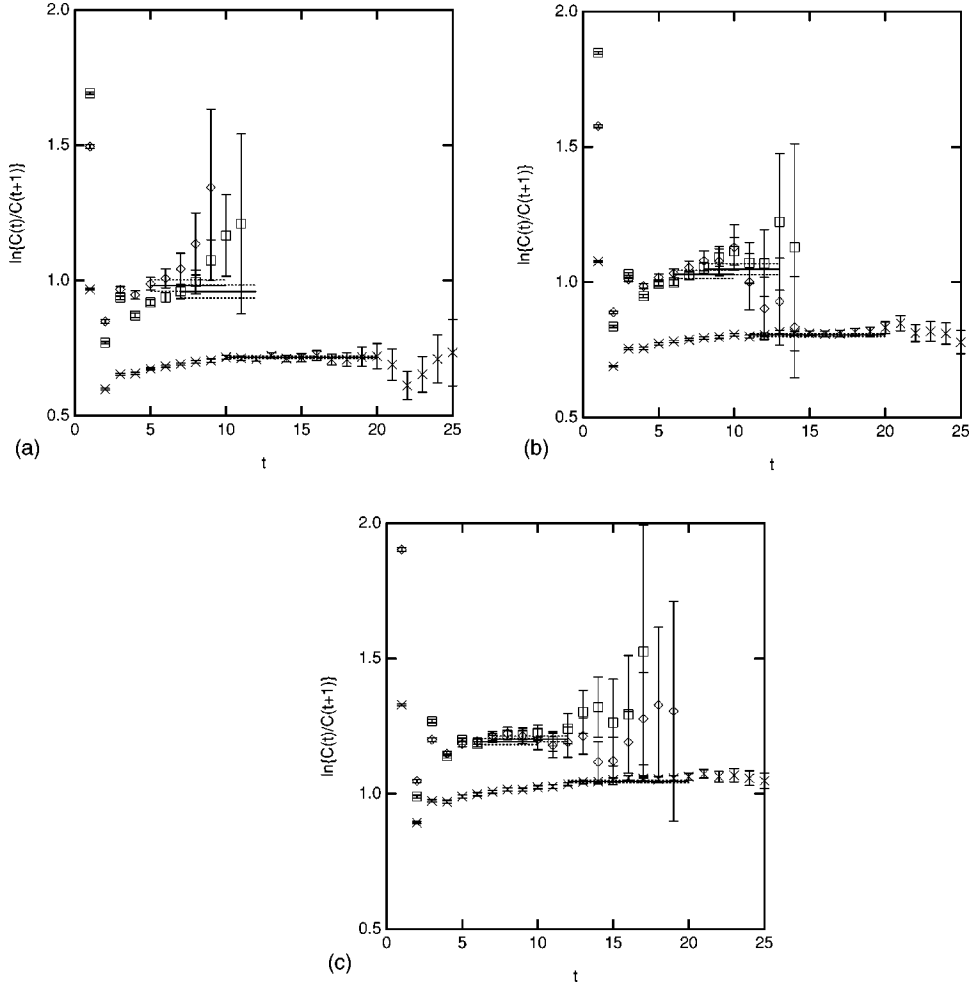
FIG. 1. (a) The effective mass of the nucleon from the $\langle\langle B_1^+(t)\bar{B}_1^+(0)\rangle\rangle$ correlator ($\times$) and its parity partner from $\langle\langle B_1^-(t)\bar{B}_1^-(0)\rangle\rangle$ ($\square$) and $\langle\langle B_2^-(t)\bar{B}_2^-(0)\rangle\rangle$ ($\diamond$) correlators on an ensemble of 405 configurations at $m_f = 0.03$. The solid lines and dashed lines represent each fitted mass and its statistical error. (b) The effective mass of the nucleon from the $\langle\langle B_1^+(t)\bar{B}_1^+(0)\rangle\rangle$ correlator ($\times$) and its parity partner from $\langle\langle B_1^-(t)\bar{B}_1^-(0)\rangle\rangle$ ($\square$) and $\langle\langle B_2^-(t)\bar{B}_2^-(0)\rangle\rangle$ ($\diamond$) correlators on an ensemble of 305 configurations at $m_f = 0.05$. The solid lines and dashed lines represent each fitted mass and its statistical error. (c) The effective mass of the nucleon from the $\langle\langle B_1^+(t)\bar{B}_1^+(0)\rangle\rangle$ correlator ($\times$) and its parity partner from $\langle\langle B_1^-(t)\bar{B}_1^-(0)\rangle\rangle$ ($\square$) and $\langle\langle B_2^-(t)\bar{B}_2^-(0)\rangle\rangle$ ($\diamond$) correlators on an ensemble of 105 configurations at $m_f = 0.10$. The solid lines and dashed lines represent each fitted mass and its statistical error.

TABLE II. Single exponential fit of the nucleon two-point correlator $\langle\langle B_1^+(t)\bar{B}_1^+(0)\rangle\rangle$ at $\beta = 6.0$ on a $16^3 \times 32 \times 16$ lattice with $M_5 = 1.8$. The systematic error is estimated from the change in the fitted mass when $t_{\min}$ is increased by one. The masses for $am_f < 0.05$ agree within errors with those given in Ref. [12] which were calculated from different correlation functions on a slightly different set of configurations.

State (J^P)	am_f	aM_N(stat)(syst)	χ^2/N_{DF}	$t_{\min}$	$t_{\max}$	Conf. level	No. of configs.
N ($1/2^+$)	0.020	0.654(12)(14)	1.00	12	20	0.43	405
	0.030	0.716(5)(0)	1.09	10	20	0.37	405
	0.040	0.754(6)(1)	1.08	11	20	0.38	305
	0.050	0.805(5)(2)	1.17	11	20	0.31	305
	0.075	0.929(7)(4)	0.81	12	20	0.58	105
	0.100	1.045(5)(3)	0.94	12	20	0.47	105
	0.125	1.162(6)(4)	0.84	15	20	0.50	105

TABLE III. Single exponential fit of the negative-parity nucleon two-point correlator $\langle\langle B_1^-(t)\bar{B}_1^-(0)\rangle\rangle$ at $\beta=6.0$ on a $16^3\times 32\times 16$ lattice with $M_5=1.8$. The systematic error is estimated from the change in the fitted mass when $t_{\min}$ is increased by one.

State (J^P)	am_f	aM_{N*}(stat)(syst)	χ^2/N_{DF}	$t_{\min}$	$t_{\max}$	Conf. level	No. of configs.
N^* ($1/2^-$)	0.020	0.935(34)(40)	1.29	6	10	0.28	405
	0.030	0.959(24)(24)	1.16	7	12	0.33	405
	0.040	1.018(28)(56)	1.49	8	12	0.22	305
	0.050	1.048(20)(38)	1.26	8	13	0.28	305
	0.075	1.104(13)(18)	1.27	7	13	0.27	105
	0.100	1.203(10)(12)	0.99	7	12	0.41	105
	0.125	1.303(8)(8)	0.92	7	12	0.45	105

ing meson mass ratio, toward the experimental values [15]. We did not include the charm sector ($M_D/M_{D*}\simeq 0.93$) since the parity partner of $\Sigma_c^{++}(2455)$ is not measured experimentally. On the other hand, from our results we estimate the mass of this state to be roughly 2.7 GeV (we have used a simple linear in the quark mass ansatz to extract the mass from our degenerate quark data).

Finally, we evaluate the N and N^* masses in the chiral limit. Taking a simple linear extrapolation in the four lightest quark masses for B_1^+ and B_1^-, we find $M_N=0.57(1)$ and $M_{N*}=0.85(5)$ in lattice units. Setting the scale from the calculated ρ-meson mass [12], we obtain $M_N\approx 1.1$ GeV and $M_{N*}\approx 1.6$ GeV in the chiral limit. If we use the scale set by the calculated nucleon mass, we obtain $M_{N*}\approx 1.5$ GeV. Either way the N^* mass is in good agreement with the experimental values within about 5–10 %. The above errors do not include systematic uncertainties due to finite volume, non-zero lattice spacing, and quenching effects. Studies of such systematic errors will be addressed in future calculations.

Recently it was suggested [40] that the N^* propagator in quenched QCD may exhibit non-analytic chiral behavior associated with the anomalous contribution of the "η'-N" intermediate state.[2] This suggestion is inspired by recent articles [41,42]. However, non-analytic effects which arise in the vicinity of the massless quark limit are hard to detect in our data since our calculation is not very close to this limit. In addition, such subtle effects could easily be mimicked by finite volume effects. The volume used in our study is still rather small. Furthermore, the statistical errors in our study are large enough, especially for the N^*, that complicated fits beyond a naive linear one would not yield meaningful parameters or χ^2.

C. Unconventional nucleon operator

As mentioned earlier, the unconventional operator B_2^+ vanishes in the non-relativistic limit, so one may expect that

---

[2]Recall that in the quenched approximation the η' is also a pseudo Goldstone boson. We stress that the quenched "η'-N" intermediate state would give a *negative metric* contribution corresponding to a "quenched chiral loop" artifact [41]. Needless to say, this spurious intermediate state, which is a source of unitarity violation, is not associated with the physical decay process [41].

it couples with negligible weight to the nucleon ground state near this limit. Indeed, no one has succeeded in extracting the ground state mass signal from $\langle\langle B_2^+(t)\bar{B}_2^+(0)\rangle\rangle$ in lattice QCD [28,26]. Then, we expect that an approximately zero overlap on the ground state provides the possibility of direct access to the excited state using the B_2^+ operator. This prospect should hold as long as the lattice operator has the same symmetries as the continuum one.

In the massless quark limit, the combinations $B_1^+\pm B_2^+$ do not mix due to different chiral structure. In perturbation theory, each is multiplicatively renormalized with the same renormalization factor so that B_1^+ and B_2^+ also do not mix. However, conventional lattice fermions give rise to mixing through explicit chiral symmetry breaking [29]. Thus, B_2^+ will couple to the ground state through unwanted mixing with B_1^+. On the other hand, the explicit breaking of chiral symmetry in domain wall fermions is highly suppressed, so there is hope that we may extract the positive-parity excited state of the nucleon from B_2^+ as the asymptotic state.

Let us first compare the effective mass plots of $\langle\langle B_1^+(t)\bar{B}_1^+(0)\rangle\rangle$ and $\langle\langle B_2^+(t)\bar{B}_2^+(0)\rangle\rangle$ correlators [see Figs. 4(a)–4(c)]. The correlator $\langle\langle B_2^+(t)\bar{B}_2^+(0)\rangle\rangle$ is considerably noisier so that only time slices near the source are useful. Nevertheless, the effective mass from $\langle\langle B_2^+(t)\bar{B}_2^+(0)\rangle\rangle$ yields a plateau albeit with large statistical errors. The plateau becomes more satisfactory for heavier quark mass. These plateaus are obviously different from those extracted from the B_1^+ correlator. When we apply the single exponential fit to the two-point correlation function composed of B_2^+, we obtain a mass that is quite large compared to the mass extracted from $\langle\langle B_1^+(t)\bar{B}_1^+(0)\rangle\rangle$ as listed in Table V. In [20] similar results from the B_2^+ correlator have been found.

As mentioned earlier, an explanation of the above result [15] is that B_2^+ has negligible overlap with the nucleon ground state since it does not have a non-relativistic limit and thus provides a direct signal for the positive-parity excited state of the nucleon. Of course, this explanation is valid only in the heavy valence-quark mass limit.

We investigate further the possibility that $\langle 0|B_2^+|N\rangle\approx 0$ through the calculation of the mixed correlation function $\langle\langle B_1^+(t)\bar{B}_2^+(0)+B_2^+(t)\bar{B}_1^+(0)\rangle\rangle$. If it is true that the overlap with the nucleon $\langle 0|B_2^+|N\rangle$ becomes small with increasing

TABLE IV. Single exponential fit of the negative-parity nucleon two-point correlator $\langle\langle B_2^-(t)\bar{B}_2^-(0)\rangle\rangle$ at $\beta=6.0$ on a $16^3\times32\times16$ lattice with $M_5=1.8$. The systematic error is estimated from the change in the fitted mass when $t_{\min}$ is increased by one.

State (J^P)	am_f	aM_{N*}(stat)(syst)	χ^2/N_{DF}	$t_{\min}$	$t_{\max}$	Conf. level	No. of configs.
$N*$ $(1/2^-)$	0.030	0.982(21)(15)	1.10	5	10	0.35	405
	0.040	0.993(16)(17)	0.81	5	10	0.52	305
	0.050	1.029(15)(16)	1.00	6	10	0.39	305
	0.075	1.092(12)(10)	0.75	5	11	0.59	105
	0.100	1.193(11)(16)	0.82	6	12	0.54	105
	0.125	1.308(13)(9)	0.84	7	15	0.55	105

valence-quark mass, mass estimates from the mixed correlator $\langle\langle B_1^+(t)\bar{B}_2^+(0)+B_2^+(t)\bar{B}_1^+(0)\rangle\rangle$ should be consistent with the nucleon for lighter quark mass and the positive-parity excited state for heavier quark mass. Such behavior is evident in Fig. 5. We stress that the single particle fit to the mixed correlation function does not in general yield the mass of an asymptotic state, only in the limits discussed above, which is clear from the figure. We also note that for improved Wilson fermions the mixed correlation function yields the ground state mass for all quark masses, even heavy ones [20]. Thus it appears in that case that there is still significant mixing of B_1^+ and B_2^+.

As a result, it is possible to identify B_2^+ with the positive-parity excited nucleon (N') for heavy quarks (e.g., $m_f \gtrsim 0.075$ in our study) [15]. Indeed, we see $|\langle 0|B_2^+|N\rangle/\langle 0|B_2^+|N'\rangle|^2 \lesssim 10^{-3}$ from double exponential fits for $\langle\langle B_2^+(t)\bar{B}_2^+(0)\rangle\rangle$ at $m_f=0.10$ and 0.125. Of course, this feature weakens in the lighter quark mass region (from around $m_f=0.05$). However, even for $m_f<0.075$, mass estimates from B_2^+ are still considerably larger than the nucleon mass, so we cannot rule out the possibility that B_2^+ provides a signal for the positive-parity excited nucleon at even lighter quark mass values.

D. Diagonalization method for 2×2 matrix correlator

Let us consider the N' in more detail. The mass of the excited nucleon may be obtained from a two state fit to the B_1^+ correlator which, however, requires large statistics and that neither the ground state or the first excited state lies close to any other state. Attempts to extract the N' mass

using this method have failed to reproduce the observed mass [25]. In our fits the Hessian matrix often becomes singular, so we cannot extract the excited state mass from double exponential fits. Instead, we take an alternative approach proposed in [43]. First, we define the 2×2 matrix correlator $\mathcal{C}(t)$ using the two distinct baryon operators

$$\mathcal{C}(t)=\begin{bmatrix} c_{11}(t) & c_{12}(t) \\ c_{21}(t) & c_{22}(t) \end{bmatrix}, \tag{24}$$

where $c_{ij}(t)=\langle\langle B_i^\pm(t)\bar{B}_j^\pm(0)\rangle\rangle$. Next we write $C(t)$ in terms of a transfer matrix $\lambda(t,t_0)$,

$$\mathcal{C}(t)\psi=\lambda(t,t_0)\mathcal{C}(t_0)\psi, \tag{25}$$

where t_0 is fixed and $t>t_0$. If only two states are propagating in a given system, the masses of the two states E_α ($E_1 >E_0$) are given by the eigenvalues of the transfer matrix:

$$\lambda_\alpha(t,t_0)=e^{-(t-t_0)E_\alpha} \quad (\alpha=0,1), \tag{26}$$

where E_α is independent of t_0. The smaller eigenvalue (λ_1) and larger eigenvalue (λ_0) refer to the masses of the excited state and the ground state respectively. In general, the system may have more than two states. Thus, we assume that two states become effectively dominant for an appropriately large time-slice t_0, which can be determined by checking the sensitivity of E_α with respect to variations of t_0.

We calculate the eigenvalues $\lambda_\alpha(t,t_0)$ of $\mathcal{C}(t_0)^{-1}\mathcal{C}(t)$ for $t_0=3$, and then evaluate the effective masses of N and N' from the larger and smaller eigenvalues, respectively, with the statistical errors coming from the jack-knife method. Us-

TABLE V. Single exponential fit of the unconventional nucleon two-point correlator $\langle\langle B_2^+(t)\bar{B}_2^+(0)\rangle\rangle$ at $\beta=6.0$ on a $16^3\times32\times16$ lattice with $M_5=1.8$. The systematic error is estimated from the change in the fitted mass when $t_{\min}$ is increased by one.

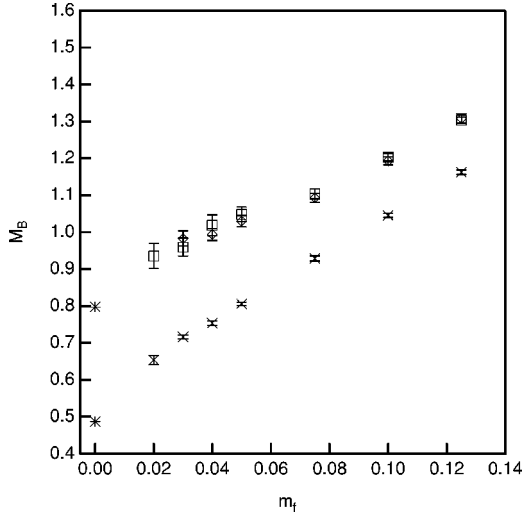| State (J^P)	am_f	$aM_{N'}$(stat)(syst)	χ^2/N_{DF}	$t_{\min}$	$t_{\max}$	Conf. level	No. of configs.
N' $(1/2^+)$	0.030	1.170(50)(108)	1.47	5	8	0.23	405
	0.040	1.191(36)(69)	1.28	5	11	0.27	305
	0.050	1.244(43)(148)	1.49	6	11	0.20	305
	0.075	1.303(39)(58)	0.43	6	10	0.73	105
	0.100	1.387(19)(2)	0.63	5	10	0.64	105
	0.125	1.484(16)(6)	1.00	5	11	0.42	105

FIG. 2. N ($\times$) and N^* ($\square$ and $\diamond$) masses versus the quark mass m_f in lattice units [$a^{-1} \approx 1.9$ GeV from $aM_\rho = 0.400(8)$ in the chiral limit]. The corresponding experimental values for N and N^* are marked with lower and upper stars. The N-N^* mass splitting is clearly observed. Symbols ($\times$, $\square$ and $\diamond$) are defined as in Fig. 1.
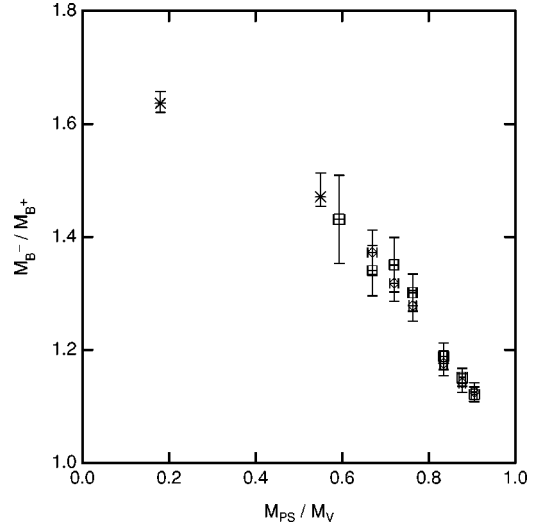

FIG. 3. Mass ratio of the negative-parity excited-state and positive-parity ground-state baryons versus mass ratio of the pseudoscalar meson and vector meson. All calculations are done for three degenerate valence quarks. Ratios are calculated using fitted masses from the $\langle\langle B_1^-(t)\bar{B}_1^-(0)\rangle\rangle$ ($\square$) and $\langle\langle B_2^-(t)\bar{B}_2^-(0)\rangle\rangle$ ($\diamond$) correlators. Experimental points are denoted by stars.

ing these error estimates, we determine the masses in Table VI from weighted averages over the time-slice ranges listed there. Figure 6 shows that the results are quite consistent with the masses determined from single exponential fits to $\langle\langle B_2^+(t)\bar{B}_2^+(0)\rangle\rangle$ and $\langle\langle B_1^+(t)\bar{B}_1^+(0)\rangle\rangle$. We have checked that the variations of t_0 around $t_0 = 3$ do not significantly affect the effective masses. For $m_f \lesssim 0.03$, we unfortunately could not extract the mass of the first excited nucleon since a good plateau in the effective mass plot is absent. We note that for $m_f = 0.04$ there is still a large splitting in the eigenvalues, indicating the overlap of B_2^+ with the nucleon remains small.

In contrast to the positive-parity state, the eigenvalues in the negative-parity case appear degenerate, as shown in Fig. 7. This will be discussed in more detail in the next section.

As we have seen, the first excited state may die out so quickly that only a few time slices are available for evaluating the mass, even if the excited state is well separated from the ground state. To circumvent this quick damping, simulations performed on an anisotropic lattice where the temporal lattice spacing is finer than the spatial one may be useful. In fact, a recent lattice study [20] has shown this to be an effective way to extract masses of nucleon excited states.

E. Comparison with experiment

In the physical spectrum, we have another negative-parity state, $N^*(1650)$, which is just above the lowest state $N^*(1535)$. Although these states are quite close to each other, they are easily distinguished due to a peculiar decay mode of $N^*(1535)$. It is well known that the decay rate of $N^*(1535) \rightarrow N + \eta$ is comparable with $N^*(1535) \rightarrow N + \pi$ even though the $N\pi$ decay mode is kinematically favored over $N\eta$. For the case of $N^*(1650)$ the $N\pi$ decay is dominant; the branching ratio of $N\eta$ is only a few percent. Thus,

$N^*(1535) \rightarrow N + \pi$ seems to be anomalously suppressed. However, the corresponding states cannot be easily distinguished without knowledge of decay patterns if they lie close to each other.

As mentioned, for the negative-parity case our data show that both eigenvalues of the transfer matrix are the same within statistical errors (see Fig. 7). Of course, this does not rule out the possibility that the splitting might become clear with more statistics and in the lighter quark mass region. That is because the central value of the difference between the two eigenvalues increases in the lighter quark mass region. Furthermore, the value of about 100 MeV at $m_f = 0.03$ seems to be large enough to reproduce experimental splitting in the chiral limit.

Nevertheless, unlike the positive-parity case, we have no indication of the presence of two independent negative-parity states in our calculation where the mixed correlator yields a consistent mass with both B_1^- and B_2^- interpolating operators, as listed in Table VI. Thus, our combined results from all data for the negative-parity nucleon allows two other possibilities regarding $N^*(1650)$. One is that $N^*(1535)$ and $N^*(1650)$ are completely degenerate or not independent in the quenched calculation. This situation resembles naive quark models and the MIT bag model where $N^*(1535)$ and $N^*(1650)$ are degenerate if we neglect the spin dependent interaction. In this case, the analysis through the diagonalization of the 2×2 correlator is no longer helpful.

A second possibility is that $N^*(1650)$ is simply missing in our calculation, i.e., both B_1^- and B_2^- operators may not couple, or couple weakly, to the $N^*(1650)$ state. This may be related to an argument in [44] where the authors show that the desired vanishing of the phenomenological πNN^* coupling for the $N^*(1535)$ state results simply from the chiral transformation properties of particular interpolating opera-
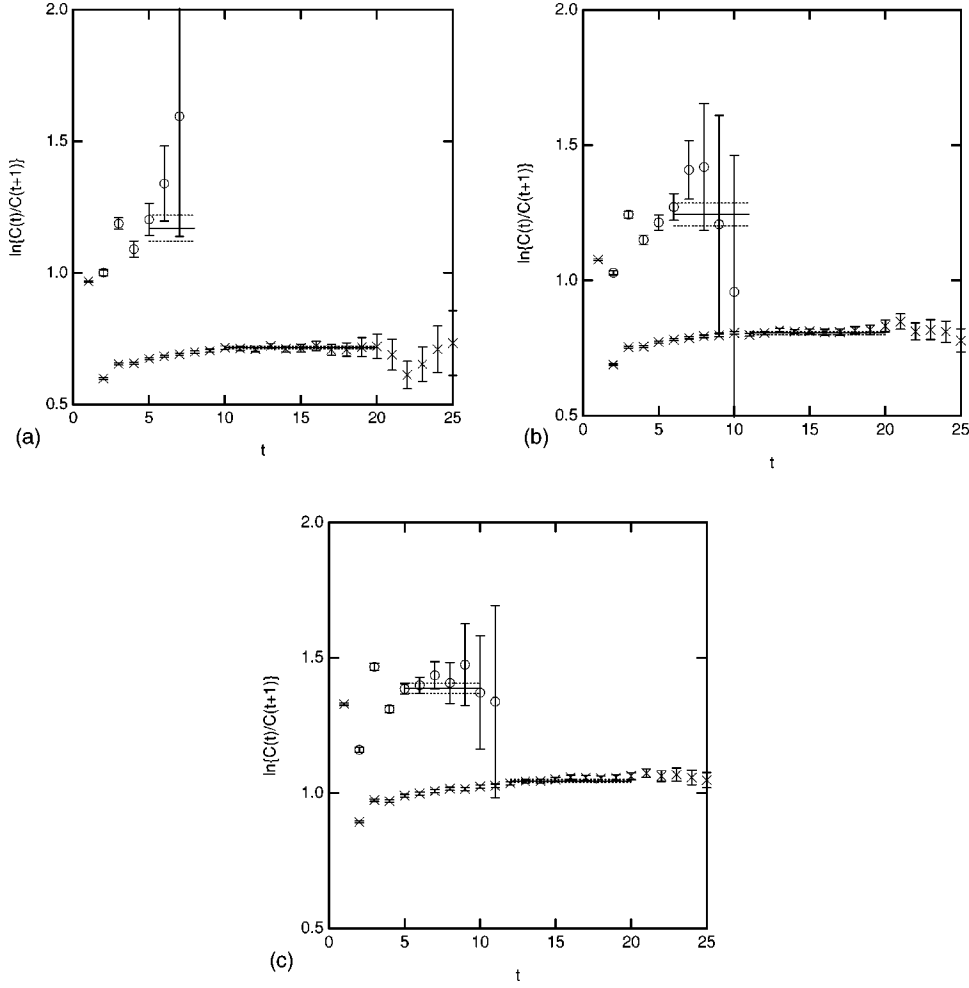
FIG. 4. (a) The effective mass from the $\langle\langle B_1^+(t)\bar{B}_1^+(0)\rangle\rangle$ ($\times$) and $\langle\langle B_2^+(t)\bar{B}_2^+(0)\rangle\rangle$ ($\bigcirc$) correlators on an ensemble of 405 configurations at $m_f=0.03$. The solid lines and dashed lines represent each fitted mass and its statistical error. (b) The effective mass from the $\langle\langle B_1^+(t)\bar{B}_1^+(0)\rangle\rangle$ ($\times$) and $\langle\langle B_2^+(t)\bar{B}_2^+(0)\rangle\rangle$ ($\bigcirc$) correlators on an ensemble of 305 configurations at $m_f=0.05$. The solid lines and dashed lines represent each fitted mass and its statistical error. (c) The effective mass from the $\langle\langle B_1^+(t)\bar{B}_1^+(0)\rangle\rangle$ ($\times$) and $\langle\langle B_2^+(t)\bar{B}_2^+(0)\rangle\rangle$ ($\bigcirc$) correlators on an ensemble of 105 configurations at $m_f=0.10$. The solid lines and dashed lines represent each fitted mass and its statistical error.

tors B_1^- and B_2^- with the help of the soft pion limit. If their argument is relevant to the suppression of the $N\pi$ decay, it is possible that B_1^- and B_2^- couple strongly to $N^*(1535)$ but not to $N^*(1650)$. However, their argument is no longer applicable to a third interpolating operator

$$B_{3\mu}^- = (u^T C\sigma_{\alpha\beta}u)\sigma_{\alpha\beta}\gamma_\mu d - (u^T C\sigma_{\alpha\beta}d)\sigma_{\alpha\beta}\gamma_\mu u, \quad (27)$$

which belongs to the chiral multiplet $(\frac{1}{2},1)\oplus(1,\frac{1}{2})$ and has no derivative [33,34]. The $B_{3\mu}^-$ couples to both $J=3/2$ and $J=1/2$ states. In this case, $N^*(1650)$ might be extracted from the $B_{3\mu}^-$ operator since there is no reason for lack of coupling to the $N^*(1650)$ state.

Finally, we would like to mention a remaining puzzle. We have done the first successful lattice calculation of both N^* and N' spectra. As for the N', we have reliable data only for relatively large values of m_f. Comparing the N' mass with the N^* mass, we find that the ordering of N' and N^* is

inverted compared to experiment. Furthermore, the level spacing between N-N^* and N^*-N' is almost even [15]. What we see here closely resembles the wrong ordering problem of the excited nucleon spectrum in naive quark models and the MIT bag model. However, if this result is true for heavy quarks, we can make an important prediction: the first excited state of the spin one-half Σ_c is a negative-parity state rather than a positive-parity state.

Unfortunately, our statistics did not allow the computation of the N' mass in the light-quark region ($m_f<0.03$). In addition, our data show no evidence for the possibility of switching the level ordering between N^* and N' towards the chiral limit. Indeed, we did not observe that the N' mass decreased faster than the N^* mass with decreasing quark mass. However, finite volume effects for higher excited states may be more serious than for lower excited states. According to naive quark models or the MIT bag model, the N' state is radially excited in contrast to the nucleon ground state and the N^* state. We note that the trend in the three
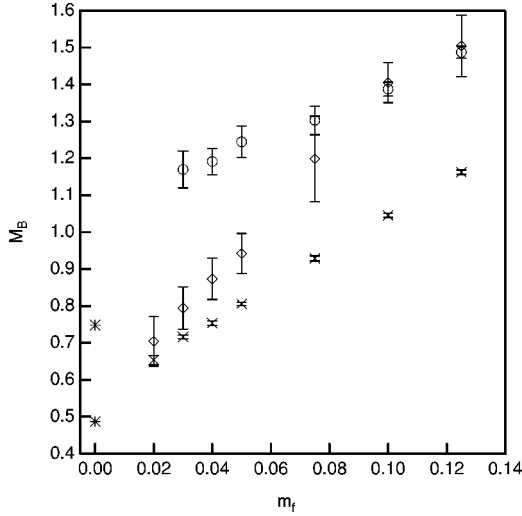
FIG. 5. The fitted mass from $\langle\langle B_1^+(t)\bar{B}_1^+(0)\rangle\rangle$ ($\times$), $\langle\langle B_2^+(t)\bar{B}_2^+(0)\rangle\rangle$ ($\bigcirc$) and mixed type $\langle\langle B_1^+(t)\bar{B}_2^+(0) + B_2^+(t)\bar{B}_1^+(0)\rangle\rangle$ ($\diamond$) correlators. The corresponding experimental values for N and N' are marked with lower and upper stars. Note, the values extracted from the mixed correlation function do not represent the mass of an actual asymptotic state, except possibly in the light and heavy quark limits.

heaviest quark mass points is at least consistent with the switching of the ordering in the chiral limit. Needless to say, the quenched approximation may also play a role in this puzzle. In summary, our results do not rule out the possibility of switching the ordering between N^* and N' near the chiral limit, and to solve this remaining puzzle we need further systematic calculations toward the chiral limit.
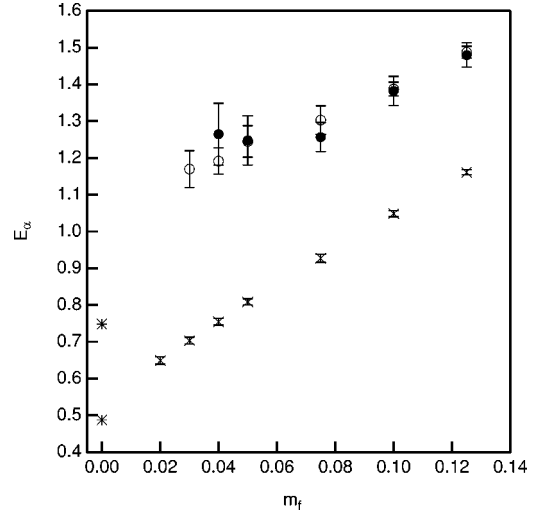

FIG. 6. Comparison of the fitted mass from $\langle\langle B_2^+(t)\bar{B}_2^+(0)\rangle\rangle$ ($\bigcirc$) and the estimated mass from the average effective mass of the smaller eigenvalue of the transfer matrix ($\bullet$). The symbol $\times$ corresponds to the nucleon ground-state mass evaluated from the larger eigenvalue of the transfer matrix, which is quite consistent with the fitted mass from $\langle\langle B_1^+(t)\bar{B}_1^+(0)\rangle\rangle$.

V. CONCLUSION

We have studied the mass spectrum of the parity partner of the nucleon in quenched lattice QCD using domain wall fermions which preserve chiral symmetry to a high degree in lattice simulations. Most importantly we demonstrated that this method is capable of calculating the mass of the negative-parity N^* state in the spin one-half and isospin one-half baryon sector.
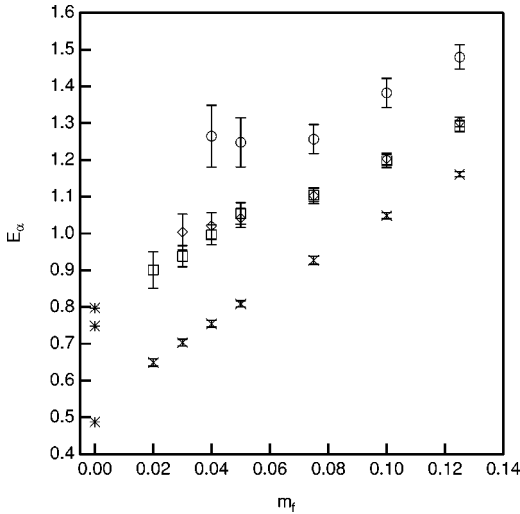
TABLE VI. The third column lists the fitted masses of the mixed type correlators. Fifth and seventh columns list the weighted averages of the effective mass derived from the larger eigenvalue and the smaller eigenvalue of the transfer matrix $\lambda_a(t,t_0=3)$ induced by the 2×2 matrix correlator. The fits corresponding to column three all have $\chi^2/N_{DF}<1.5$ For the positive-parity state, the larger and smaller eigenvalue of the transfer matrix are clearly distinguishable. They correspond to the nucleon ground state (N) and the first excited nucleon (N') respectively. However, for the negative parity state, both eigenvalues are degenerate within errors.

J^P	am_f	Mixed type	$[t_{min},t_{max}]$	E_0	$[t_{min},t_{max}]$	E_1	$[t_{min},t_{max}]$	No. of configs.
$1/2^+$	0.020	0.704(67)	[6,11]	0.649(10)	[6,13]	N/A		200
	0.030	0.795(57)	[5,12]	0.703(9)	[7,15]	N/A		200
	0.040	0.873(56)	[5,12]	0.755(9)	[7,20]	1.264(84)	[5,8]	200
	0.050	0.942(54)	[5,11]	0.808(8)	[8,20]	1.247(67)	[5,10]	200
	0.075	1.198(115)	[5,10]	0.927(11)	[11,20]	1.256(39)	[4,10]	81
	0.100	1.405(54)	[3,10]	1.048(9)	[12,20]	1.382(39)	[5,10]	81
	0.125	1.504(83)	[4,10]	1.161(7)	[13,20]	1.479(33)	[5,10]	81
$1/2^-$	0.020	N/A		0.901(50)	[5,10]	N/A		200
	0.030	0.992(47)	[5,11]	0.938(29)	[5,10]	1.004(49)	[4,10]	200
	0.040	0.979(24)	[5,11]	0.996(27)	[6,10]	1.021(35)	[5,10]	200
	0.050	1.005(16)	[5,11]	1.054(29)	[7,11]	1.042(26)	[5,11]	200
	0.075	1.092(14)	[5,12]	1.105(18)	[5,10]	1.102(22)	[5,10]	81
	0.100	1.185(10)	[5,10]	1.197(18)	[5,12]	1.203(16)	[5,12]	81
	0.125	1.282(9)	[5,11]	1.292(16)	[5,12]	1.303(13)	[5,12]	81

FIG. 7. Symbols $\square$ and $\diamond$ correspond to the estimated mass from the average effective mass of the larger and smaller eigenvalues of the transfer matrix for the negative parity state. The eigenvalues are degenerate within errors. Symbols $\times$ and $\bigcirc$ are defined as in Fig. 6. The corresponding experimental values for $N(939)$, $N'(1440)$ and $N^*(1535)$ are marked with lower, middle and upper stars. The ordering of the negative-parity nucleon (N^*) and the positive-parity excited nucleon (N') is inverted relative to experiment.

We made a systematic investigation of the N^* spectrum by using two distinct interpolating operators, B_1^- and B_2^-. We found the N^* mass estimates extracted from them agree with each other. In practice the B_1^- correlator is more convenient than B_2^- in extracting the N^* mass because it is less noisy, especially in the light quark mass region.

We have found a definite mass splitting between N and N^* states in the whole quark mass range we studied. Furthermore, this splitting grows with decreasing quark mass. The N^* mass and the N-N^* mass splitting in the chiral limit obtained by extrapolation are consistent with the experimental value within about 5–10 %, depending on the mass we choose to set the lattice spacing, the nucleon or the ρ meson. These results have been confirmed by subsequent lattice calculations using improved Wilson fermions [20,21]. Needless to say this is very encouraging for further investigations of N^* physics using lattice QCD simulations.

In contrast to the negative parity operators, the positive parity operators, B_1^+ and B_2^+, yield distinct mass signals. From the B_1^+ operator we obtained a clean signal for the nucleon ground state, while from B_2^+ we always found a heavier mass. This is probably because the latter vanishes in the non-relativistic limit and thus has small overlap with the ground state. Indeed, we confirmed numerically that $\langle 0|B_2^+|N\rangle \simeq 0$ and that B_2^+ yields the mass signal of the positive-parity excited state in the heavy quark region. We found that in the heavy quark mass region the mass of this excited state is about twice as high above the ground state mass as the N^* mass. This property of the B_2^+ operator was confirmed by comparing the results with the excited-state spectrum obtained from the diagonalization of a 2×2 corre-

lation matrix constructed from both interpolating operators and also by examining single particle fits to the mixed correlation function.

We did not resolve a long-standing puzzle regarding the excited-state spectrum of the nucleon, the inversion of the positive- and negative-parity first excited states with respect to experiment. However, we believe that the level switching between N^* and N' must occur close to the chiral limit, though there is scant evidence in our results that this might happen. Taking our calculation at face value leads to the prediction that the first excited state of Σ_c has $J^P = 1/2^-$.

Needless to say, more work needs to be accomplished in order to achieve a fully systematic calculation of the excited nucleon spectrum. In the near future we plan to increase our volume and statistics to further explore the chiral limit, and to check that lattice spacing errors are small by running at several gauge couplings. We expect that the latter effect is small due to the chiral symmetry properties of domain wall fermions. A long term goal is to include dynamical fermions.

APPENDIX: GENERAL CHIRAL TRANSFORMATION AND PARITY PARTNERS

To extend our discussion of Sec. III C to general chiral transformations, we prepare iso-doublet operators for B_1^+ and B_2^+,

$$\mathcal{B}_1^+(x) = \begin{pmatrix} \varepsilon_{abc}[u_a^T(x)C\gamma_5 d_b(x)]u_c(x) \\ \varepsilon_{abc}[d_a^T(x)C\gamma_5 u_b(x)]d_c(x) \end{pmatrix}, \quad \text{(A1)}$$

$$\mathcal{B}_2^+(x) = \begin{pmatrix} \varepsilon_{abc}[u_a^T(x)Cd_b(x)]\gamma_5 u_c(x) \\ \varepsilon_{abc}[d_a^T(x)Cu_b(x)]\gamma_5 d_c(x) \end{pmatrix}. \quad \text{(A2)}$$

The upper component corresponds to the proton and the lower component corresponds to the neutron. Also we can define iso-doublet operators for the negative parity nucleons as $\mathcal{B}_{1,2}^- = \gamma_5 \mathcal{B}_{1,2}^+$, respectively. Here we consider a general transformation of $SU(2)_V$ and $SU(2)_A$ symmetry,

$$[\mathcal{Q}_V^a, q(x)] = i\tau_a q(x), \quad \text{(A3)}$$

$$[\mathcal{Q}_A^a, q(x)] = i\tau_a \gamma_5 q(x), \quad \text{(A4)}$$

where $q=(u,d)^T$ and τ_a is a Pauli matrix. Under these transformations, the two-point correlator composed of either $\mathcal{B}_1^\pm$ or $\mathcal{B}_2^\pm$ should transform as

$$[\mathcal{Q}_V^a,\mathcal{B}_{1,2}^\pm(x)\bar{\mathcal{B}}_{1,2}^\pm(0)]=i[\tau_a,\mathcal{B}_{1,2}^\pm(x)\bar{\mathcal{B}}_{1,2}^\pm(0)], \quad (A5)$$

$$[\mathcal{Q}_A^a,\mathcal{B}_{1,2}^\pm(x)\bar{\mathcal{B}}_{1,2}^\pm(0)]=i\{\gamma_5\tau_a,\mathcal{B}_{1,2}^\pm(x)\bar{\mathcal{B}}_{1,2}^\pm(0)\}. \quad (A6)$$

Equation (A5) along with the fact that $\mathcal{Q}_V^a|0\rangle=0$ tells us that the nucleon two-point correlation function should be commute with τ_a,

$$[\tau_a,G_{\mathcal{B}^\pm}(t)]=0, \quad (A7)$$

which means that $G_{\mathcal{B}^+}(t)$ has only diagonal elements of iso-spin indices. In other words, the proton state and the neutron state are eigenstates of iso-spin, of course. If $\mathcal{Q}_A^a|0\rangle=0$, it turns out that

$$\{\gamma_5\tau_a,G_{\mathcal{B}^\pm}(t)\}=\tau_a\{\gamma_5,G_{\mathcal{B}^\pm}(t)\}=0. \quad (A8)$$

Thus, we can obtain the strict relation in terms of two-point correlators between the nucleon and its parity partner

$$G_{\mathcal{B}^+}(t)=G_{\mathcal{B}^-}(t) \quad (A9)$$

in the non-broken phase of chiral symmetry.

[1] S. Aoki *et al.*, Phys. Rev. Lett. **84**, 238 (2000).
[2] S. Kim and S. Ohta, Phys. Rev. D **61**, 074506 (2000).
[3] C. Bernard *et al.*, Phys. Rev. Lett. **81**, 3087 (1998).
[4] H.B. Nielsen and M. Ninomiya, Nucl. Phys. **B185**, 20 (1981); **B195**, 541(E) (1982); **B193**, 173 (1981).
[5] M.F.L. Golterman and J. Smit, Nucl. Phys. **B255**, 328 (1985).
[6] D. Kaplan, Phys. Lett. B **288**, 342 (1992).
[7] Y. Shamir, Nucl. Phys. **B409**, 90 (1993).
[8] V. Furman and Y. Shamir, Nucl. Phys. **B439**, 54 (1995).
[9] R. Narayanan and H. Neuberger, Phys. Rev. Lett. **71**, 3251 (1993); Phys. Lett. B **302**, 62 (1993).
[10] T. Blum and A. Soni, Phys. Rev. Lett. **79**, 3539 (1997); Phys. Rev. D **56**, 174 (1997).
[11] An early review of domain wall fermions is given in T. Blum, Nucl. Phys. B (Proc. Suppl.) **73**, 167 (1999); For a recent review, see P. Vranas, *ibid.* **94**, 177 (2001).
[12] T. Blum *et al.*, Phys. Rev. D (to be published), hep-lat/0007038.
[13] A. Ali Khan *et al.*, Phys. Rev. D **63**, 114504 (2001).
[14] See, e.g., H. Pagels, Phys. Rep. **16**, 219 (1975).
[15] S. Sasaki, Nucl. Phys. B (Proc. Suppl.) **83**, 206 (2000); S. Sasaki, in *Proceedings of the International Conference on NSTAR 2000, Newport News, VA, 2000*, edited by V.D. Burkert *et al.* (World Scientific, Singapore, 2001), p. 378, hep-ph/0004252.
[16] T. Blum, S. Ohta, and S. Sasaki, Nucl. Phys. B (Proc. Suppl.) **94**, 295 (2001).
[17] S. Güsken, K. Schilling, R. Sommer, K.-H. Mütter, and A. Patel, Phys. Lett. B **212**, 216 (1988).
[18] T. Bhattacharya, R. Gupta, G. Kilcup, and S. Sharpe, Phys. Rev. D **53**, 6486 (1996).
[19] F.X. Lee and D.B. Leinweber, Nucl. Phys. B (Proc. Suppl.) **73**, 258 (1999).
[20] F.X. Lee, Nucl. Phys. B (Proc. Suppl.) **94**, 251 (2001).
[21] D.G. Richards, Nucl. Phys. B (Proc. Suppl.) **94**, 264 (2001).
[22] N. Isgur and G. Karl, Phys. Rev. D **19**, 2653 (1979).
[23] A. Chodos *et al.*, Phys. Rev. D **10**, 2599 (1974).
[24] L.Ya. Glozman and D.O. Riska, Phys. Rep. **268**, 263 (1996).
[25] S. Cabasino *et al.*, Phys. Lett. B **258**, 195 (1991); Y. Iwasaki *et al.*, Phys. Rev. D **53**, 6443 (1996).
[26] D.B. Leinweber, Phys. Rev. D **51**, 6383 (1995).
[27] C. Allton and S. Capitani, Nucl. Phys. **B526**, 463 (1998).
[28] K.C. Bowler *et al.*, Nucl. Phys. **B240**, 213 (1984).
[29] D. Richards *et al.*, Nucl. Phys. **B286**, 683 (1987).
[30] S. Aoki *et al.*, Phys. Rev. D **60**, 114504 (1999).
[31] T. Blum, A. Soni, and M. Wingate, Phys. Rev. D **60**, 114507 (1999).
[32] For example, see R.G. Edwards and U. Heller, Phys. Rev. D **63**, 094505 (2001); P. Hernandez, K. Jansen, and M. Lüscher, hep-lat/0007015; F. Berruto, R. Narayanan, and H. Neuberger, Phys. Lett. B **489**, 243 (2000); and Y. Shamir, Phys. Rev. D **62**, 054513 (2000).
[33] B.L. Ioffe, Nucl. Phys. **B188**, 317 (1981).
[34] T.D. Cohen and X. Ji, Phys. Rev. D **55**, 6870 (1997).
[35] F. Fucito *et al.*, Nucl. Phys. **B210**, 407 (1982).
[36] G. 't Hooft, in *Recent Developments in Gauge Theories*, edited by 't Hooft *et al.* (Plenum, New York, 1980); S. Coleman and B. Grossman, Nucl. Phys. **B203**, 205 (1982).
[37] N. Christ (private communication).
[38] L. Wu, Nucl. Phys. B (Proc. Suppl.) **83**, 224 (2000); M. Wingate, *ibid.* **83**, 221 (2000).
[39] Particle Data Group, C. Caso *et al.*, Eur. Phys. J. C **3**, 1 (1998).
[40] M. Göckeler *et al.*, hep-lat/0106022.
[41] W. Bardeen *et al.*, Phys. Rev. D **65**, 014509 (2002).
[42] C. Bernard *et al.*, Phys. Rev. D **64**, 054506 (2001).
[43] M. Lüscher and U. Wolff, Nucl. Phys. **B339**, 222 (1990).
[44] D. Jido, M. Oka, and A. Hosaka, Phys. Rev. Lett. **80**, 448 (1998).